

Inhibition of oxidative phosphorylation underlies the antiproliferative and proapoptotic effects of mofarotene (Ro 40-8757) in Burkitt's lymphoma cells

Roberta Cariati¹, Paola Zancai¹, Elisabetta Righetti³, Silvana Rizzo¹, Anita De Rossi³, Mauro Boiocchi^{*2} and Riccardo Dolcetti¹

¹Immunovirology and Biotherapy Unit, Italy; ²Division of Experimental Oncology I, Department of Pre-clinical and Epidemiological Research, Centro di Riferimento Oncologico, IRCCS – National Cancer Institute, Aviano (PN), Italy; ³Department of Oncology and Surgical Sciences, AIDS Reference Center, Padova, Italy

In the search for retinoids active against Burkitt's lymphoma (BL), we found that the arotinoid mofarotene (Ro 40-8757) induced strong antiproliferative and apoptotic responses in most established BL cell lines as well as in primary BL cells. Ro 40-8757-induced apoptosis is associated with mitochondrial membrane depolarization, activation of caspase-3 and -9, and enhanced production of reactive oxygen species. These effects were related to a transient drop in intracellular ATP content, probably favored by a downregulation of NADH dehydrogenase subunit-1, a component of the mitochondrial respiratory chain (MRC) Complex I. Inhibition of MRC with thenoyltrifluoroacetone suppressed both the ATP recovery and apoptosis, confirming that the effects of Ro 40-8757 are mediated by changes in mitochondrial function. Compared to EBV-negative lines, EBV-carrying BLs were more resistant to Ro 40-8757-induced apoptosis. EBV infection and ectopic LMP-1 expression increased the resistance of BL cells to Ro 40-8757-induced apoptosis, probably through bcl-2 upregulation. Finally, we also show that 2-methoxyoestradiol, an inhibitor of the scavenger enzymes superoxide dismutases, enhanced Ro 40-8757-mediated apoptosis. These findings provide the rationale for evaluating the clinical efficacy of Ro 40-8757 in BL patients and suggest that the combination of Ro 40-8757 with inhibitors of scavenger enzymes may be a promising therapeutic approach for this aggressive lymphoma.

Oncogene (2003) 22, 906–918. doi:10.1038/sj.onc.1206060

Keywords: Burkitt's lymphoma; retinoids; Ro 40-8757; Epstein–Barr virus; reactive oxygen species; oxidative phosphorylation

Introduction

Burkitt's lymphoma (BL) is the most common type of childhood non-Hodgkin's lymphoma (50%), being less

frequent in immunocompetent adults (2%) (Hecht and Aster, 2000). On the basis of differences in geographic distribution, two major subgroups of BL can be distinguished: an endemic form, which is restricted to some regions of equatorial Africa and New Guinea, and a sporadic form, which occurs worldwide (Hecht and Aster, 2000). Recently, the incidence of sporadic BL has markedly increased, mainly as a consequence of human immunodeficiency virus-related immunosuppression (Knowles *et al.*, 1988). Although all BLs are characterized by the presence of reciprocal translocations activating the *c-myc* gene, the two BL types differ in terms of association with EBV (Hecht and Aster, 2000). In fact, while nearly all endemic BLs carry the EBV genome, only a proportion of sporadic BLs is linked to EBV infection, with prevalence values ranging from 10 to 85% in different areas (Hecht and Aster, 2000). The disease is highly aggressive, often showing a very rapid course with bulky abdominal masses, and frequent bone marrow, central nervous system, and extranodal involvement (White *et al.*, 1992). Clinical experience has shown that BL can be effectively controlled only by dose-intensive combination chemotherapy regimens similar to those used for acute lymphoblastic leukemias (Morrison and Peterson, 1999). Although some improvement has been recently achieved by strategies including bone marrow transplantation, a proportion of patients show a recurrence of the disease that is no longer responsive to treatment (Morrison and Peterson, 1999). On these grounds, new therapeutic options need to be explored in BL patients, particularly in those with refractory relapse.

Retinoids, the natural and synthetic derivatives of vitamin A, regulate a broad spectrum of biological processes and are considered promising agents for the prevention and treatment of human cancer. In particular, all-*trans*-retinoic acid (ATRA) induced complete remission in most patients with acute promyelocytic leukemia (Fenaux *et al.*, 1997). Moreover, recent results have indicated that retinoids, alone or in combination with other drugs, may also have some activity in other hematological malignancies, including juvenile chronic myeloid leukemia (Castleberry *et al.*, 1994), myelodysplastic syndrome (Ohno, 1994), and cutaneous T cell lymphoma (French *et al.*, 1994). Nevertheless, the

*Correspondence: M Boiocchi, Division of Experimental Oncology I, Centro di Riferimento Oncologico, IRCCS, National Cancer Institute, via Pedemontana Occidentale 12, 33081 Aviano (PN), Italy; E-mail: mboiocchi@cro.it

Received 25 January 2002; revised 18 September 2002; accepted 24 September 2002

possible efficacy of retinoids in the control of B-cell lymphoproliferations has been scarcely explored.

To provide the *in vitro* bases that could support the use of these compounds in the management of B-cell lymphoproliferative disorders, we have recently characterized the biological effects exerted by several retinoids on B-cell lines representative of various stages of lymphomagenesis. In particular, we have shown that 13-*cis*-RA, 9-*cis*-RA, and ATRA exert a strong and persistent antiproliferative effect on EBV-immortalized LCLs at concentrations corresponding to therapeutically achievable plasma levels (Pomponi *et al.*, 1996). Similar effects were also induced in LCLs carrying an activated *c-myc* oncogene (Cariati *et al.*, 2000). In contrast, RA exerted significant antiproliferative responses only in a minority of BL cell lines, inducing a growth arrest that was fully reversible upon drug removal (Cariati *et al.*, 2000). In the search for retinoids active against BL, we found that the arotinoid mofarotene (Ro 40-8757) was able to markedly inhibit the growth of BL cells but not of EBV-immortalized LCLs. The present study was aimed at characterizing the effects exerted by Ro 40-8757 on BL cell growth and survival in the light of the possible use of this compound for the treatment of BL. In particular, we herein show that Ro 40-8757 exerts strong antiproliferative and apoptotic responses in both established cell lines and primary cell cultures derived from BL patients. These effects are probably mediated by inhibition of oxidative phosphorylation at the level of complex I of the mitochondrial respiratory chain (MRC), which ultimately result in the enhanced generation of reactive oxygen species (ROS). Moreover, we also demonstrate that the proapoptotic effects of Ro 40-8757 may be enhanced by the combined use of inhibitors of radical-scavenging intracellular antioxidants, providing thus a rational background to verify the *in vivo* efficacy of schedules including Ro 40-8757 in the management of BLs.

Results

Ro 40-8757 inhibits BL cell growth

The arotinoid Ro 40-8757 was able to markedly inhibit (> 50% at 1 μ M for 3 days) the proliferation of six

(Akata, Daudi, Ramos, Raji, Namalwa, and BL-41) of the eight BL cell lines investigated (not shown). Proliferation of DG 75 cells was only minimally decreased, whereas P3HR1 cells were completely resistant to the antiproliferative activity of this compound (not shown). Responsiveness to Ro 40-8757-mediated growth inhibition was not correlated with the ethnic origin of the primary BL, the type of *c-myc*-activating translocation, and EBV status. The antiproliferative effect was further investigated by the analysis of dose-response curves of Daudi and Ramos cells treated with drug concentrations ranging from 0.01 to 10 μ M. In both cell lines, Ro 40-8757 induced a dose-dependent decrease in ³H-thymidine uptake starting from day 2 and becoming more pronounced after 7 days of treatment (Figure 1). Of note, the antiproliferative effect exerted by Ro 40-8757 in these cell lines was evident also at low drug concentrations (up to 0.03 μ M) (Figure 1). Moreover, the drug induced a marked dose-dependent antiproliferative effect also in short-term cell cultures derived from a patient with BL in the leukemic phase (CS-BL) (Figure 1).

Effects of Ro 40-8757 on cell cycle

Analysis of cell cycle distribution of Daudi, Raji, Ramos, BL41, and CS-BL cells treated for 3 days with 10 μ M Ro 40-8757 showed variable accumulations of cells in the S or G₀/G₁ phases (Table 1). Conversely, no evident cell cycle perturbation was observed in BL cells exposed to lower drug concentrations (1 μ M) (Table 1), despite the reduction in ³H-thymidine uptake (Figure 1 and not shown). To better understand the antiproliferative effects of Ro 40-8757, particularly those induced by low drug concentrations, Ramos and Daudi cells were further investigated by 5-bromo-2'-deoxy-uridine (BrdU) incorporation and propidium iodide (PI) staining. After 24 h of treatment with 1 μ M Ro 40-8757 or the solvent alone, cells were labeled with BrdU for 30 min and then chased by incubation for lengthening intervals. While control cells efficiently progressed through all phases of the cell cycle, Ro 40-8757-treated cells cycled more slowly (Figure 2). In fact, at 7 h, BrdU-labeled/high PI Ro 40-8757-treated Daudi cells were still in the S phase, whereas control cultures already appeared in the G₁ phase after completion of mitosis.

Table 1 Distribution of BL cells among cell cycle phases after Ro 40-8757 treatment

	Raji			Ramos			Daudi			BL41			CS-BL (short-term culture)		
	DMSO	Ro 40-8757		DMSO	Ro 40-8757		DMSO	Ro 40-8757		DMSO	Ro 40-8757		DMSO	Ro 40-8757	
		1 μ M	10 μ M		1 μ M	10 μ M		1 μ M	10 μ M		1 μ M	10 μ M		1 μ M	10 μ M
Pre-G ₀ /G ₁	2	8	13	8	25	39	9	10	10	31	43	73	11	13	20
G ₀ /G ₁	36	39	47	34	58	12	42	49	48	32	39	NE	57	51	38
S	35	34	30	44	34	88	29	22	29	46	42	NE	36	40	56
G ₂ /M	39	27	23	22	8	0	29	29	23	22	19	NE	7	9	6

Cells were treated with 1 or 10 μ M Ro 40-8757 or DMSO. Data are relative to a 24-h treatment for Raji, Ramos, Daudi, and BL41 BL cell lines and to 5 days of treatment for short-term cultures obtained from the CS patient (CS-BL). The percentage of cells in the relative cell cycle phase is shown. Cell cycle phase distribution of BL41 cells treated with 10 μ M Ro 40-8757 could not be evaluated because of high rates of apoptosis (NE: not evaluable). Results of one representative experiment of three are shown.

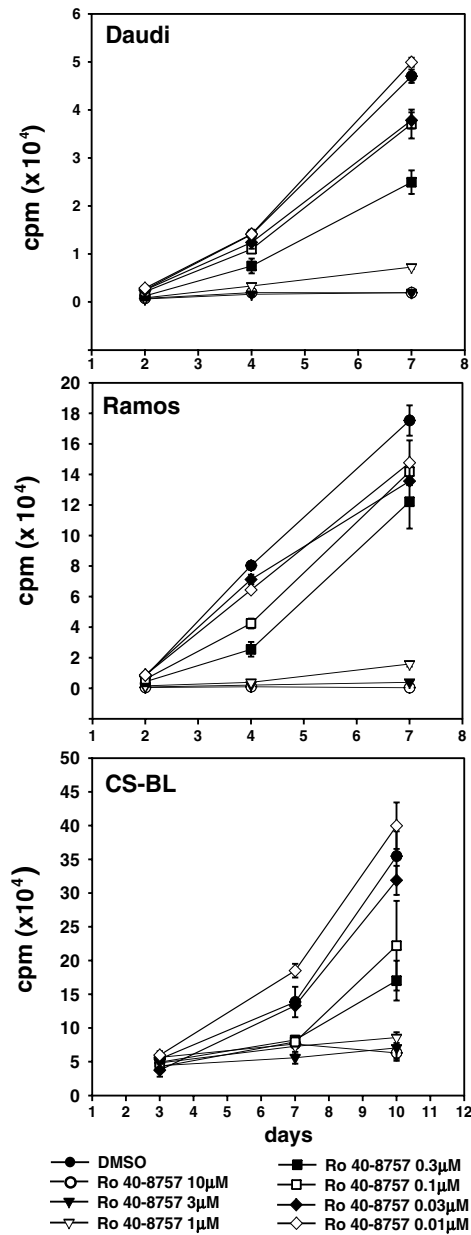


Figure 1 Ro 40-8757 induces dose-dependent antiproliferative effects in BL cells. Dose-response curves were obtained in Daudi and Ramos BL cell lines and in the short-term CS-BL cell cultures. Cell proliferation was evaluated at the indicated time points in cells treated with Ro 40-8757 concentrations ranging from 0.01 to 10 μM. The results of one representative experiment out of three are shown. Each point represents the mean ± s.d. of values obtained from triplicate wells

Moreover, unlike control cultures, only a small percentage of Ro 40-8757-treated, BrdU-labeled cells had finished semiconservative DNA synthesis after 12–16 h (Figure 2). The analysis of Ramos cells gave comparable results (not shown). Consistently, quantification of the time of DNA synthesis, showed that Ro 40-8757-treated cells had a markedly longer S phase compared with controls: 45 vs 12 h for Daudi, and 24 vs 9 h for Ramos.

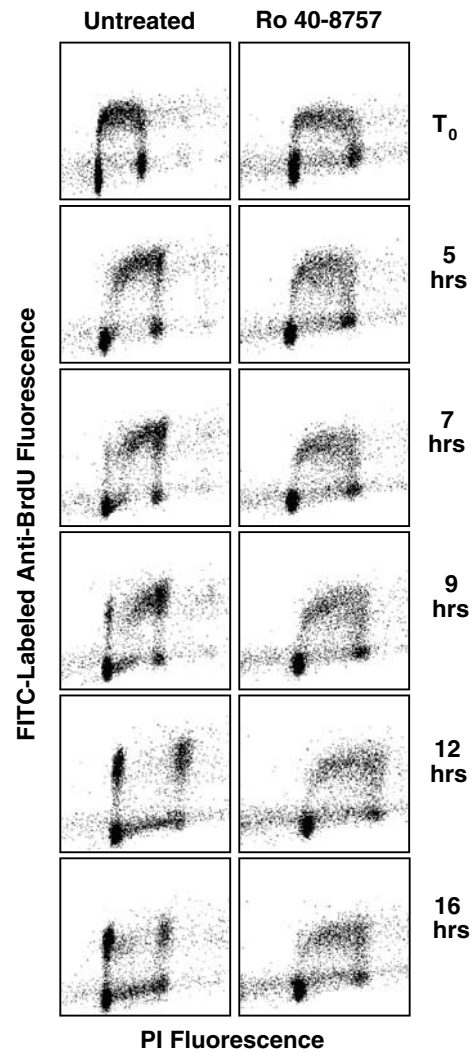


Figure 2 BrdU pulse-chase labeling demonstrating that Ro 40-8757 decreases the rates of BL cell progression through the cell cycle. While untreated-Daudi cells efficiently progressed through all phases of the cell cycle, Ro 40-8757-treated cells cycled more slowly. In fact, at 7 h, BrdU-labeled/high PI cells from control cultures already appeared in the G₁ phase after completion of mitosis. In contrast, only a small percentage of Ro 40-8757-treated, BrdU-labeled cells recycled to G₁, being the majority of these cells still being in the S phase at 16 h. Daudi cells were treated for 24 h with 1 μM Ro 40-8757 or the solvent alone. The cells were pulse-labeled with BrdU for a 30-min period and pulse-chased thereafter. Cell cultures were harvested at the indicated time after BrdU pulse. Similar findings were obtained with Ramos cells

Induction of apoptosis by Ro 40-8757

To verify whether Ro 40-8757-mediated BL cell growth inhibition was associated with the induction of apoptosis, Daudi, Raji, Ramos, and BL41 cells were investigated for the appearance of sub-G₁ populations after treatment with 10 μM or 1 μM Ro 40-8757. At the lower drug concentration, increased apoptotic rates were observed in Ramos and BL41, but not in Daudi and Raji cells, whereas at 10 μM a significant increase in the number of hypodiploid cells was detected in all four cell

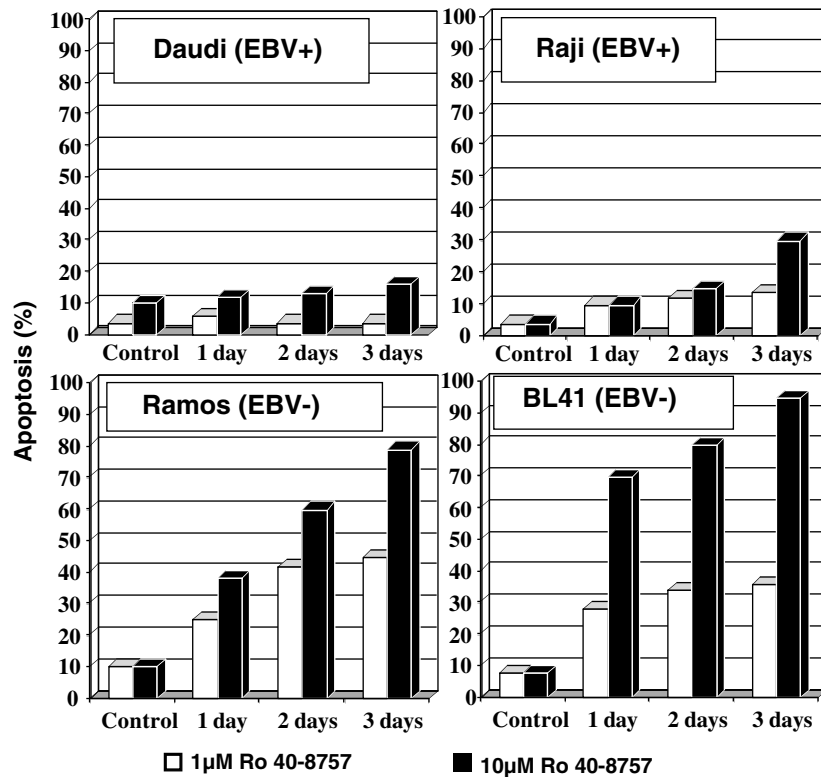


Figure 3 Ro 40-8757 induced a dose-dependent increase in the number of apoptotic BL cells. Percentage of apoptotic cells was determined on PI-stained cells by flow cytometry in Daudi, Raji, Ramos, and BL41 cells. The entity of Ro 40-8757-induced apoptosis was higher in EBV-negative BL cell lines compared to EBV-carrying lines. The cells were cultured in the presence of 1 or 10 μM Ro 40-8757, harvested at the indicated time points, and apoptosis was measured by determining the percentage of nuclei gating below the G_1 fluorescence relative to the total number of nuclei. C = control cultures treated with the solvent alone

lines (Table 1 and Figure 3). Nevertheless, the increase in sub- G_1 populations induced by 10 μM Ro 40-8757 varied depending on the cell line investigated, being low for EBV-carrying BLs (Daudi, 0–25%; Raji, 10–30%) and higher for EBV-negative (BL41, 70–90%; Ramos, 50–80%) cell lines (Figure 3). Similar proapoptotic effects were detected with the TUNEL assay (not shown). The possibility that EBV infection could increase the resistance to Ro 40-8757-mediated apoptosis was investigated in more detail by analyzing the effects of Ro 40-8757 in BL41 cells stably infected with the B95.8 strain of EBV and compared their apoptotic response with that of the parental cell line. As shown in Figure 4a, the BL41-B95.8 revertant cell line was almost completely resistant to Ro 40-8757-induced apoptosis, a phenomenon that was related to a marked upregulation of bcl-2 protein expression (Figure 4b). Moreover, ectopic expression of the EBV-encoded LMP-1 gene in the (EBV-negative) BJAB cells resulted in a marked upregulation of bcl-2 protein and in a dramatic loss of sensitivity of these cells to Ro 40-8757-induced apoptosis (Figure 4a and c).

A slight but significant increase in the number of pre- G_0/G_1 apoptotic cells was observed also in the CS-BL short-term cultures after treatment with 10 μM Ro 40-8757 for 3 days (Table 1).

Ro 40-8757 alters mitochondrial membrane potential and activates the mitochondria-mediated caspase cascade

BL cells treated with Ro 40-8757 were further characterized for alterations of the mitochondrial transmembrane potential, which is an important marker of mitochondria involvement during the apoptotic process. Therefore, Ramos cells were treated with 10 μM Ro 40-8757 for 7, 24, and 48 h, stained with the cationic dye MitoSensorTM, and analyzed by flow cytometry. While no change was observed after 7 h, a decrease in the number of cells accumulating the probe in the mitochondria (red fluorescence) was evident at 24 h and became more pronounced after 48 h of treatment (Figure 5a). At this time point, in fact, the decrease in red fluorescent cells induced by Ro 40-8757 was paralleled by a concomitant increase in the number of cells showing a green fluorescence only, consistent with the retention of the dye in the cytoplasm as a likely consequence of altered mitochondrial transmembrane potential (Figure 5a).

To assess whether Ro 40-8757-induced BL cell apoptosis involves the activation of a caspase cascade, Ramos and Daudi cells were treated for 48 h with 10 μM Ro 40-8757 and analyzed for caspase-3(-like) activity using the DEVD-pNA substrate. As shown in Figure 5b,

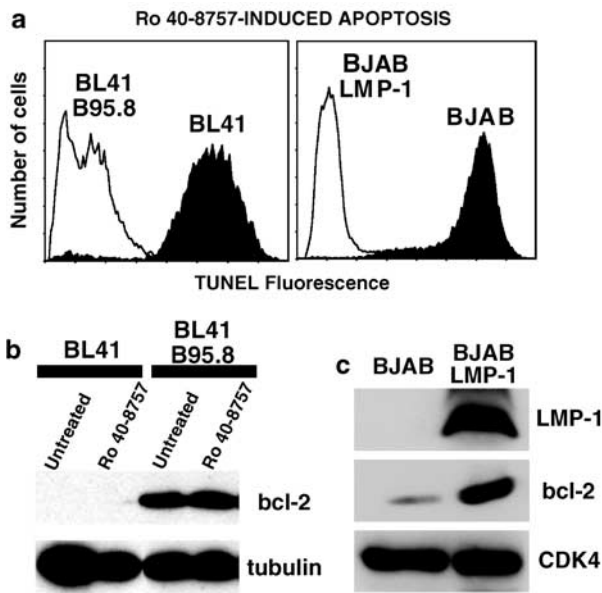


Figure 4 (a) EBV infection of the highly responsive BL41 cell line (left panel) and LMP-1 transfection of BJAB cells (right panel) resulted in an almost complete resistance to Ro 40-8757-induced apoptosis, as shown by TUNEL assay and flow cytometry analysis. The results of one representative experiment out of three are shown. (b) EBV infection of BL41 cells is associated with upregulation of the bcl-2 protein. Treatment with Ro 40-8757 did not affect the bcl-2 protein levels in the BL41-B95.8 cell line. (c) The EBV-encoded LMP-1 gene is directly responsible for bcl-2 upregulation in BJAB cells. As a loading control, the same membranes were stripped and reprobbed with antibodies to tubulin (b) and CDK-4 (c)

exposure to Ro 40-8757 was associated with enhanced caspase-3(-like) activity in both cell lines, although the increase was more pronounced in Ramos than in Daudi cells (3.5- vs 1.8-fold induction), consistently with the different responsiveness to Ro 40-8757-mediated apoptosis of these cell lines. Moreover, treatment with Ro 40-8757 also induced an increase in caspase-9(-like) activity, which was abrogated by the specific inhibitor LEHD-CHO (Figure 5b). These findings are consistent with a likely involvement of mitochondria in Ro 40-8757-mediated BL cell apoptosis.

Antiproliferative and proapoptotic effects exerted by Ro 40-8757 in BL cell lines are associated with downregulation of NADH dehydrogenase subunit 1 (ND1) gene expression

In some carcinoma cell lines, the antiproliferative activity of Ro 40-8757 was related to the ability of the drug to affect mitochondrial gene expression. In particular, Ro 40-8757 was reported to downregulate the gene encoding for ND1, an enzyme belonging to the complex I of the MRC (Uchida *et al.*, 1994). To verify whether Ro 40-8757 has similar effects in BL cells, ND1 mRNA levels were investigated in Daudi, Ramos, Raji, and BL41 cell lines treated with 10 or 1 μ M Ro 40-8757 for 7, 13, and 24 h. In all BL lines investigated, Northern blot analysis showed a marked downregulation of ND1

mRNA, which was more pronounced and stable over time at higher drug concentrations (Figure 6a). In particular, at 24 h, the ND1 mRNA levels remained stably low in Daudi and Raji cells treated with 10 μ M Ro 40-8757, while at this time point Ramos and BL41 cells showed a slight recovery of ND1 mRNA expression (Figure 6a). In contrast, no significant change in the ND1 mRNA levels was detected in the HDE-14 LCL, consistent with the resistance of these cells to the antiproliferative and proapoptotic effects of Ro 40-8757 (not shown). Downregulation of ND1 mRNA induced by the drug is an early event, being detectable after 2 h of treatment (Figure 6c). Consistent with the effects on ND1 gene transcription, Ro 40-8757 also induced a marked decrease in the levels of the ND1 protein, as shown in Ramos cells after 24 h treatment (10 μ M) (Figure 6b).

Effects of Ro 40-8757 on intracellular ATP content

To gain further insights into the mechanisms by which Ro 40-8757 inhibits the growth and induces apoptosis in BL cells, the effects of this drug on intracellular ATP levels were investigated in BL41, Ramos, and Raji cells. Consistent with the downregulation of ND1 mRNA, in all three cell lines, Ro 40-8757 induced a dose-dependent decrease in ATP content during the first 12 h of treatment followed by a recovery of ATP levels between 12 and 24 h, with peak values 1.4–2.2-fold higher than the basal levels (Figure 7a and data not shown). To verify whether Ro 40-8757-induced apoptosis is dependent on the ATP recovery, we investigated whether depletion of reducing equivalents for MRC could inhibit Ro 40-8757-mediated ATP recovery and, consequently, BL cell apoptosis. To this end, BL cells were treated with 10 μ M Ro 40-8757 in the presence of theoniltri-fluoroacetone (TTFA), an inhibitor of succinate dehydrogenase, an enzyme constituting MRC Complex II, which is also a key intermediate of the tricarboxylic acid cycle. As shown in Figure 7a, TTFA (1 mM), markedly reduced or completely inhibited the ATP recovery induced by Ro 40-8757 in Raji, BL41 and Ramos cells. Moreover, 24-h treatment with 10 μ M Ro 40-8757 in the presence of TTFA induced a 40–50% reduction of TUNEL-positive apoptotic cells in the Ramos and BL41 cells (not shown). These findings were analyzed in more detail with Annexin V/PI double staining, which showed that treatment with 10 μ M Ro 40-8757 and 1 mM TTFA for 24 h induced a shift from apoptosis (Annexin V-labeled cells) to necrosis (Annexin V/PI-labeled cells) in Ramos cells (Figure 8a). Consistent with the results of TUNEL experiments, TTFA significantly decreased Ro 40-8757-induced apoptosis also in BL41 cells (Figure 8a). Nevertheless, at the same time point, in BL41 cells, TTFA induced a shift towards viable cell compartment (Annexin V/PI-unlabeled cells) (Figure 8a), whereas the number of necrotic cells increased only later (data not shown). These results support the hypothesis that Ro 40-8757-induced apoptosis is dependent on the ATP recovery that follows the initial transient drop in ATP levels.

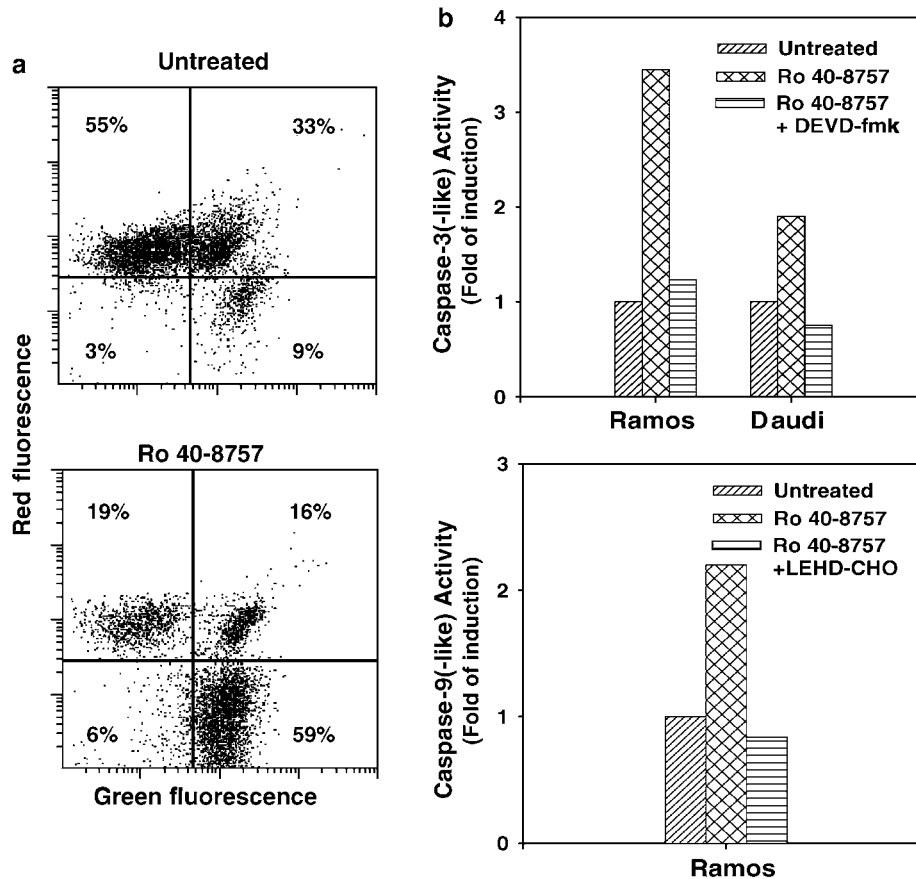


Figure 5 (a) Ro 40-8757 induces a loss of mitochondrial membrane potential in BL cells. Ramos cells were treated for 48 h with 10 μ M Ro 40-8757 and stained with the cationic dye MitoSensor™, which, in healthy cells, is taken up in the mitochondria where it forms aggregates exhibiting red fluorescence. Treatment with Ro 40-8757 induced a decrease in red fluorescent Ramos cells that occurred concomitantly with an increase in the number of cells showing a green fluorescence only, consistent with the retention of the dye in the cytoplasm as a likely consequence of altered mitochondrial transmembrane potential. The fluorescence emitted by cells was analyzed by flow cytometry. (b) Ro 40-8757 induces caspase-3(-like) and caspase-9(-like) activity in BL cells. Upper panel: Ramos and Daudi cells (2×10^6) were treated for 2 days with 10 μ M Ro 40-8757 or the solvent alone. Caspase-3(-like) activity was measured using the DEVD-pNA substrate. Specificity of caspase-3 activation was evaluated by adding the CPP32 inhibitor DEVD-fmk. Lower panel: Ramos cells were cultured for 48 h in the presence of Ro 40-8757 (10 μ M) or DMSO. Caspase-9 activation was demonstrated by cleavage of the LEHD-AMC substrate which releases free fluorescent AMC for fluorimetric detection. To confirm the specificity of caspase-9 activation, the specific inhibitor LEHD-CHO was added before incubation with the substrate. The results of one representative experiment out of three are shown

Effects of Ro 40-8757 on lactate production

Since glycolysis contributes to the formation of ATP, we verified whether the ATP recovery was at least partly because of enhanced rates of glycolysis. To this end, we measured lactate concentration in the culture medium of BL41, Ramos, and Raji cells either untreated or exposed to 10 or 1 μ M Ro 40-8757. Recovery of ATP content in BL41 and Raji cells cannot be ascribed to increased glycolysis, since lactate levels did not change significantly during the initial 24–48 h of treatment, when the recovery of ATP levels occurs (data not shown). In contrast, in Ramos cells, 10 μ M Ro 40-8757 induced a progressive increase in the levels of lactate with values about 2.4- and 4-fold higher than controls at 1 and 2 days, respectively. Consistent with a possible contribution of glycolysis in Ramos cells is the finding that the ATP peak observed after Ro 40-8757 treatment reached markedly higher values in Ramos than in BL41 and Raji

cells (2.2- vs 1.4-fold the basal level) (Figure 7a). Overall, these results seem to rule out that an enhanced glycolysis is the major determinant of the ATP recovery observed in Ro 40-8757-treated cells, partially contributing to this phenomenon only in some BL cell lines.

Ro 40-8757-induced BL cell apoptosis is inhibited by antioxidants and is associated with enhanced ROS production

Mitochondria are the main source of ROS (Richter and Schweizer, 1997), and several reports have shown that mitochondrial ROS may be involved in the induction of apoptosis (Buttke and Sandstrom, 1994; Slater *et al.*, 1995). In particular, it has been reported that inhibition of MRC complex I not only leads to a decline in mitochondrial ATP production, but may also enhance ROS generation by the MRC (Pryor, 1982; Buttke and

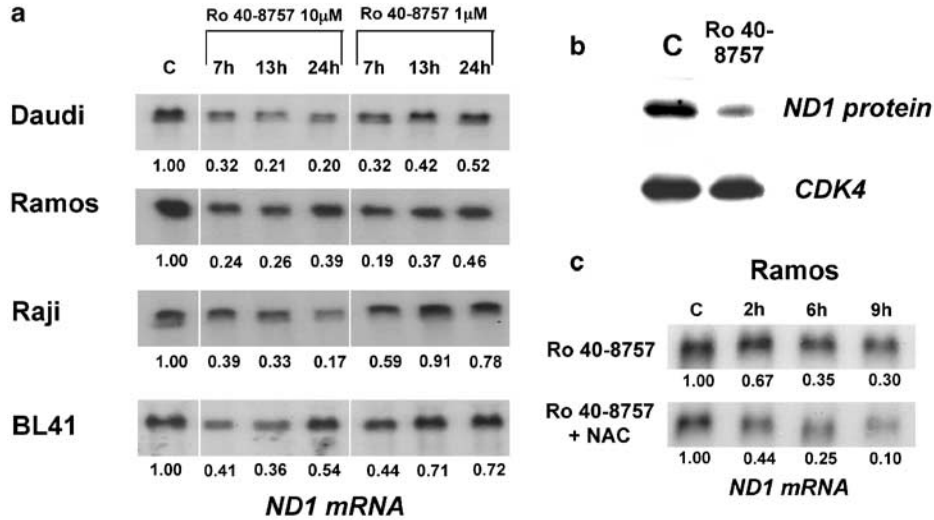


Figure 6 (a) Ro 40-8757 downregulates ND1 mRNA expression. Raji, Daudi, BL41 and Ramos cells were treated for 7, 13, and 24 h with 10 or 1 μ M Ro 40-8757. Total RNA was analyzed by Northern blotting with a specific probe to ND1 as described in Materials and methods. Numbers below each panel represent the quantification of the amounts of ND1 mRNA after normalization with 28S RNA levels, as assessed by laser densitometry. (b) Ro 40-8757 induces downregulation of ND1 protein in BL cells. Ramos cells were treated for 24 h Ro 40-8757 (10 μ M) and analyzed by immunoblotting with an anti-ND1 specific antibody. As a loading control, the same membrane was stripped and re probed with a CDK4-specific antibody. (c) Ro 40-8757-induced ND1 mRNA downregulation is not inhibited by antioxidants. Ramos cells were treated with 10 μ M Ro 40-8757 for 2, 6, and 9 h in the presence or absence of 6 mM NAC

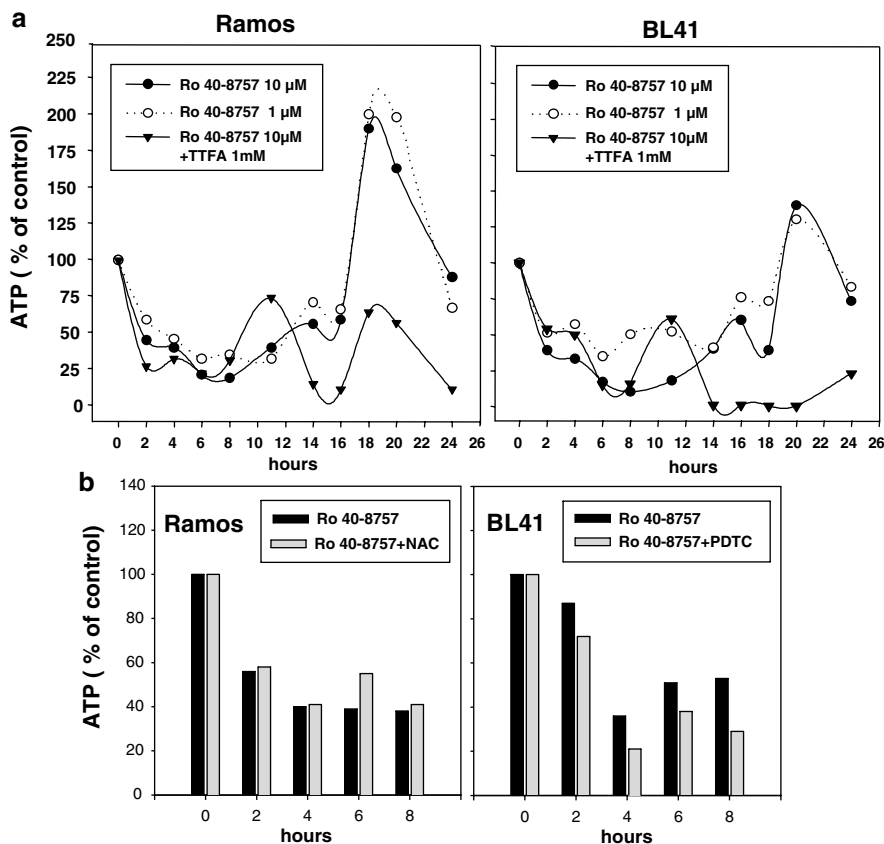


Figure 7 Effects of Ro 40-8757 on intracellular ATP content in BL cells. (a) Ramos and BL41 cells were exposed to 10 or 1 μ M Ro 40-8757 for the times indicated and then assayed for ATP content. The MRC inhibitor TTFA (1 mM) markedly reduced or completely inhibited the transient ATP recovery induced by 10 μ M Ro 40-8757. Similar findings were obtained with Raji cells (not shown). (b) Antioxidants do not inhibit the drop of ATP levels induced by 10 μ M Ro 40-8757. Ramos and BL41 cells were treated with 10 μ M Ro 40-8757 for 2, 4, 6, and 8 h in the presence or absence of antioxidants (6 mM NAC for Ramos and 70 μ M PDTC for BL41) and then analyzed for intracellular ATP levels. Results are expressed as percentage of control values. The results of one representative experiment out of three are shown

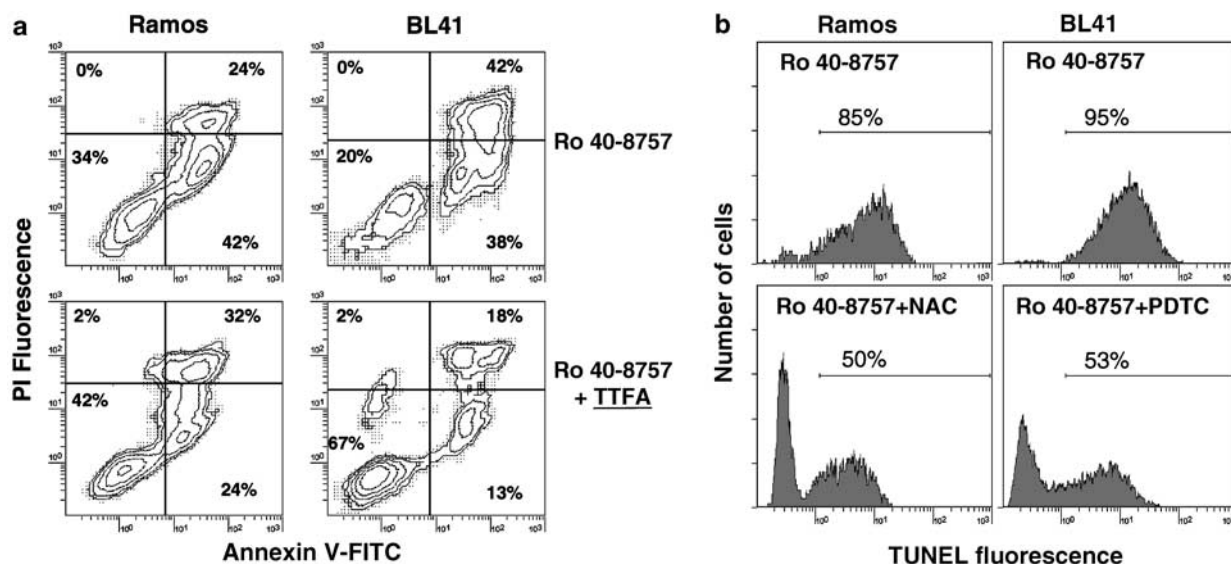


Figure 8 (a) Inhibition of MRC decreased Ro 40-8757-induced BL cell apoptosis. Dual parameter flow cytograms of FITC-labeled Annexin-V (x-axis) vs PI staining (y-axis) in Ramos and BL41 cells treated for 24 h with 10 μ M Ro 40-8757 and 1 mM TTFA or Ro 40-8757 alone. In both cell lines, TTFA significantly decreased Ro 40-8757-induced apoptosis (Annexin-V-labeled cells). A shift from apoptosis (Annexin-V-labeled cells) to necrosis (Annexin-V/PI-labeled cells) is evident in Ramos cells treated with both Ro 40-8757 and TTFA. At the same time point, TTFA induced a shift towards viable cell compartment (Annexin-V/PI-unlabeled cells), whereas the number of necrotic cells increased only later. (b) Ro 40-8757-mediated apoptosis is inhibited by antioxidants. The proapoptotic effects of 10 μ M Ro 40-8757 administered for 24 h were analyzed in Ramos and BL41 cells in the presence of 6 mM NAC or 70 μ M PDTC. Apoptosis was evaluated by TUNEL assay and flow cytometry, as described in Materials and methods. Results relative to the effects of NAC in Ramos cells and of PDTC in BL41 cells are shown. The results of one representative experiment out of three are shown

Sandstrom, 1994; Slater *et al.*, 1995). Therefore, with the aim to investigate the possible involvement of ROS in Ro 40-8757-induced BL cell apoptosis, we verified whether the antioxidants pyrrolidine dithiocarbamate (PDTC) (70 μ M), and *N*-acetyl-L-cysteine (NAC) (6 mM) were able to suppress the proapoptotic effects of 10 μ M Ro 40-8757 administered for 24 h to BL41 and Ramos cells. TUNEL experiments indicated that these antioxidants inhibited Ro 40-8757-induced apoptosis by 40–50% in both cell lines, with Ramos cells being more sensitive to NAC and BL41 cells to PDTC (Figure 8b). Consistently, Ro 40-8757 treatment enhanced ROS generation in both cell lines, as assessed by flow cytometric analysis of dihydroethidine (DHE) staining (Figure 9). The increase in ROS production occurred later than ND1 mRNA downregulation, becoming evident only after 4–6 h of treatment and was partially inhibited by antioxidants (Figure 9 and not shown). The use of the oxidation-sensitive fluorescent dye 5-(and-6)-chloromethyl-2', 7'-dichlorodihydrofluorescein diacetate (CM-H₂DCFDA) gave similar results confirming that Ro 40-8757 increases ROS generation in BL cells (not shown). Moreover, NAC was unable to inhibit Ro 40-8757-induced ND1 mRNA downregulation in Ramos cells (Figure 6b), supporting the hypothesis that the enhanced ROS generation induced by the drug is the consequence and not the cause of the decreased ND1 gene expression. Consistently, also the drop in the ATP levels induced by Ro 40-8757 in both Ramos and BL41 cells was not inhibited by antioxidants (Figure 7b), ruling out, therefore, that the observed ATP depletion might be the consequence of the enhanced ROS generation. Of

note, the progressive increase in ROS production induced by Ro 40-8757 was closely associated with a concomitant increase in the number of apoptotic cells (Figure 9), further supporting the involvement of ROS in Ro 40-8757-induced BL cell apoptosis.

Ro 40-8757-mediated apoptosis may be enhanced by inhibitors of superoxide dismutases

Our finding that the apoptosis induced by Ro 40-8757 is antioxidant-sensitive provided the basis to verify whether compounds able to impair cellular defenses against oxidative stress may enhance Ro 40-8757-induced BL cell apoptosis. To this end, we evaluated the apoptotic responses induced by Ro 40-8757 in combination with 2-methoxyestradiol (2-ME), an estrogen derivative able to inhibit superoxide dismutases (Huang *et al.*, 2000), enzymes crucial for the elimination of superoxide radicals (Fridovich, 1995). These experiments were carried out using Raji cells, in which Ro 40-8757 induced limited apoptotic responses. In these cells, 2-ME significantly enhanced the apoptotic response of 0.01 μ M Ro 40-8757 (Figure 10). Treatment with 1 μ M 2-ME alone was associated with moderate apoptotic effects, with about 30% of Annexin V-labeled apoptotic cells on day 2 (Figure 10).

Discussion

In the present study, we provide evidence that the arotinoid mofarotene (Ro 40-8757) is able to strongly

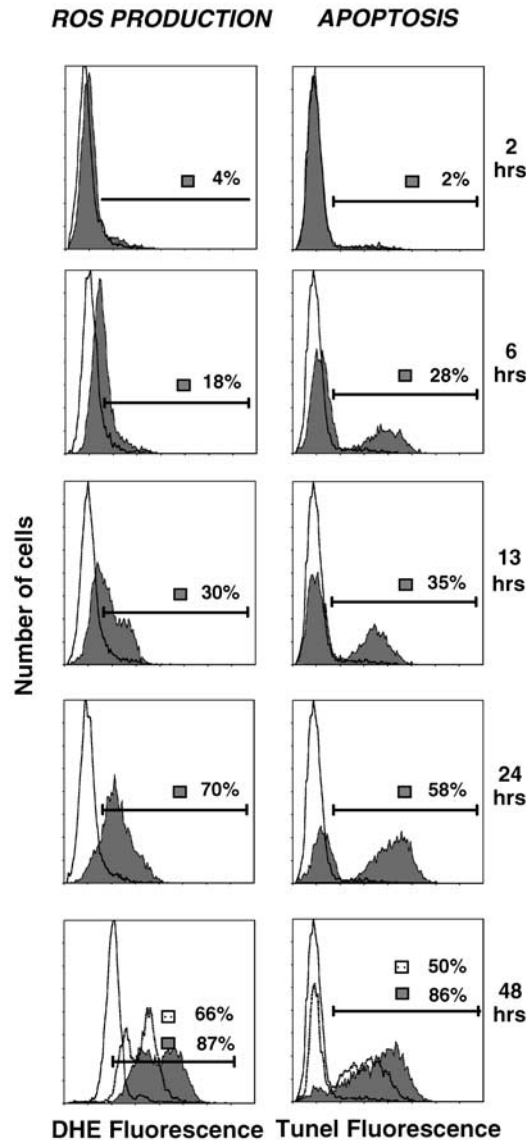


Figure 9 Ro 40-8757 enhances ROS generation in BL cells concomitantly with increased apoptotic rates. Left panel: Intracellular ROS production was evaluated by DHE labeling (■) in Ramos cells treated with 10 μ M Ro 40-8757 for 2, 6, 13, 24, and 48 h. The antioxidant NAC (6 mM) inhibited Ro 40-8757-induced ROS production, as shown in the histogram relative to 48 h of treatment (□). Similar inhibition of ROS generation by NAC was also observed at earlier time points (not shown). To evaluate ROS production, cells were incubated at 37°C for 15 min in the presence of 20 ng/ml DHE in complete medium and then immediately analyzed for fluorochrome incorporation by flow cytometry. Right panel: Aliquots of Ramos cells from the same experiment were analyzed in parallel for the number of apoptotic cells by TUNEL assay (■). In the histogram relative to 48 h of treatment, the inhibition of Ro 40-8757-induced apoptosis by 6 mM NAC is shown (□). The results of one representative experiment out of three are represented

inhibit proliferation of both established cell lines and short-term cultures derived from BLs. This compound exhibited a significant degree of activity also at relatively low concentrations and against a wide panel of BL cell lines, regardless of the geographic origin of primary

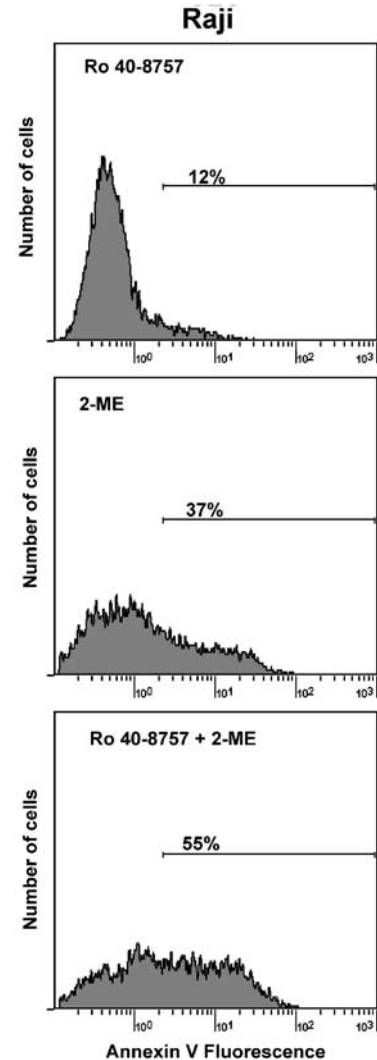


Figure 10 Ro 40-8757-mediated apoptosis may be enhanced by inhibitors of superoxide dismutases. Raji cells were treated for 2 days with 0.01 μ M Ro 40-8757 and 1 μ M 2-ME or Ro 40-8757 alone. Apoptosis was evaluated by Annexin-V labeling and flow cytometry. The results of one representative experiment out of three are shown. Similar findings were obtained with the BL41 cell line

lymphoma and the type of *c-myc*-activating translocation. These findings are in keeping with previous observations demonstrating that Ro 40-8757 was one of the most active retinoids in inhibiting the growth of a variety of cell lines derived from carcinomas of different origin (Eliason *et al.*, 1993; Uchida *et al.*, 1994; Louvet *et al.*, 1996). Moreover, consistent with what observed in other cellular systems, the drug did not induce any cell cycle phase-specific accumulation of BL cells (Eliason *et al.*, 1993; Uchida *et al.*, 1994; Louvet *et al.*, 1996). Biparametric evaluation of BrdU incorporation and DNA staining demonstrated that Ro 40-8757 induced a global lengthening of the cell cycle. In particular, the transit through the S phase was 3 to 4-fold longer after exposure to the drug.

Of note, Ro 40-8757 was also able to enhance BL cell apoptotic rates in a dose-dependent fashion, triggering a proapoptotic signaling involving loss of mitochondrial membrane potential, caspase-9 and -3 activation. Taken together, these results indicate that Ro 40-8757 induces BL cell apoptosis by a mitochondrial-mediated pathway (Kroemer and Reed, 2000). The activation of Ro 40-8757-mediated apoptotic response is apparently peculiar of BL cells, since data reported so far indicate that the drug inhibited the growth of carcinoma-derived cells without affecting their viability (Eliason *et al.*, 1993; Uchida *et al.*, 1994; Louvet *et al.*, 1996). This holds true also for non-neoplastic B lymphocytes, as we have previously shown (Pomponi *et al.*, 1996). Interestingly, we found that, like EBV-immortalized LCLs, EBV-carrying BL cell lines were also less sensitive to Ro 40-8757-mediated apoptosis compared to EBV-negative lines. The protective role of EBV with respect to Ro 40-8757-induced apoptosis was further demonstrated by the observation that EBV infection of the highly responsive BL41 cell line resulted in the induction of an almost complete resistance to Ro 40-8757-mediated apoptotic response. Similar effects were observed in BJAB cells upon transfection with the LMP-1 gene, suggesting that expression of this EBV-encoded gene alone is sufficient to confer resistance to Ro 40-8757-induced apoptosis. Consistent with what was observed in normal and transformed B lymphocytes (Henderson *et al.*, 1991; Komano *et al.*, 1999; Ruf *et al.*, 2000), both EBV infection of BL41 cells and LMP-1 transfection of BJAB cells were associated with a marked upregulation of bcl-2 protein, indicating a likely relevant role of bcl-2 in mediating the resistance to Ro 40-8757-induced BL cell apoptosis.

The mechanism of action of Ro 40-8757 is still largely unknown. Although the drug belongs to the arotinoid class of retinoids, it does not bind to or activate any of the known retinoic acid receptors (RARs) or retinoid X receptors (RXRs) (Hartmann *et al.*, 1993; Teelmann *et al.*, 1993). The antiproliferative effects induced by Ro 40-8757 in breast and pancreatic carcinoma cell lines were related to downregulation of mitochondrial gene transcription (Uchida *et al.*, 1994), although the functional consequences of this phenomenon have not been investigated so far. Besides showing that Ro 40-8757 downregulates ND1 mRNA and protein also in BL, we herein report that these effects are associated with a marked drop in intracellular ATP content occurring within the first 12h of treatment, consistent with a significant impairment of MRC complex I activity. These results suggest that inhibition of energy production by oxidative phosphorylation probably underlies the effects exerted by Ro 40-8757 on BL cell cycle, particularly the S phase lengthening and, ultimately, growth inhibition. The marked responsiveness of most BL cell lines to the antiproliferative effects of Ro 40-8757 may be, at least in part, related to the (high) energy demand of these cells because of their rapid proliferative turnover. Ro 40-8757-induced impairment of ATP production by oxidative phosphorylation may have clinically relevant effects also in normal proliferating

cells. In fact, the proposed mechanism of action of Ro 40-8757 may also underlie the reported ability of this compound to protect hematopoietic progenitor cells from cytotoxic drugs, presumably by preventing these cells from entering the cell cycle (Eliason *et al.*, 1994, 1995). These effects are fully reversible (Eliason *et al.*, 1994, 1995) and may be particularly advantageous in case of inclusion of Ro 40-8757 in the management of BL.

Consistent with recent findings indicating that inhibition of bioenergetic pathways may result in apoptosis (Richter *et al.*, 1996; Marton *et al.*, 1997), depletion of ATP content induced by Ro 40-8757 may be responsible for the proapoptotic effects exerted by the drug also in this cellular system. Since apoptosis is an active process that requires ATP (Richter *et al.*, 1996), the recovery of ATP levels observed after 12h of treatment probably constitutes a compensatory mechanism that provides the energy supply to successfully carry out the apoptotic process. Our results seem to exclude that enhanced glycolysis is the major determinant of the ATP recovery associated with Ro 40-8757-induced apoptosis, and suggest that other biochemical mechanisms, presumably involving mitochondrial pathways, probably play a major role in determining this phenomenon. This is supported by the finding that inhibition of MRC electron flow by TTFA markedly inhibits both the ATP recovery and the apoptosis induced by the drug.

Under aerobic conditions, the respiratory chain is a potent source of free radicals (Pryor, 1982; Buttke and Sandstrom, 1994; Slater *et al.*, 1995) and data from different experimental systems indicate that complex I impairment may lead to enhanced ROS production (Pitkanen and Robinson, 1996; Higuchi *et al.*, 1998; Seaton *et al.*, 1998; Barrientos and Moraes, 1999). Moreover, apoptosis may occur when the amount of ROS produced in the mitochondria cannot be handled by radical-scavenging intracellular antioxidants. Our findings indicate that increased ROS generation is a likely relevant mechanism by which Ro 40-8757 induces apoptosis in BL cells. In fact, antioxidants, such as PDTc and NAC, inhibited Ro 40-8757-induced apoptosis. Moreover, experiments carried out with two different probes (CM-H₂DCFDA and DHE) consistently indicated that the drug induced a progressive increase in ROS production, a phenomenon that occurred concomitantly with increased apoptotic rates and was partially inhibited by antioxidants. Our findings are consistent with the possibility that ND1 mRNA and protein downregulation may, at least in part, contribute the enhanced ROS generation induced by Ro 40-8757. Such a conclusion is supported by the finding that ND1 mRNA downregulation was evident since 2h of treatment, whereas the increase in ROS production occurred later (after 4h). Moreover, antioxidants were unable to inhibit both the ND1 mRNA downregulation and the drop in the ATP levels induced by Ro 40-8757. Whether ND1 is the primary target of Ro 40-8757 or whether changes affecting other mitochondrial and/or cellular genes are also involved in mediating the effects of this arotinoid remains to be elucidated.

Besides its strong antiproliferative activity, also the proapoptotic properties shown by Ro 40-8757 in this cellular system are of potential therapeutic relevance. Nevertheless, the entity of apoptotic responses induced by the drug in BL cells was heterogeneous, with a proportion of cell lines showing only limited increases in apoptotic rates. Our finding that Ro 40-8757-mediated apoptosis is antioxidant-sensitive prompted us to verify whether modalities able to decrease cellular defenses against oxidative stress may enhance the apoptosis induced by the drug in BL cells. To this purpose, we investigated the proapoptotic effects of the combination of Ro 40-8757 with 2-ME, an estradiol derivative that was recently found to induce apoptosis in leukemic but not in normal lymphocytes by inhibiting superoxide dismutases (Huang *et al.*, 2000), essential enzymes that protect from damage induced by superoxide radicals (Fridovich, 1995). Here we demonstrate that 2-ME enhanced Ro 40-8757-mediated apoptosis, particularly in BL cell lines showing limited apoptotic responses after treatment with Ro 40-8757 alone. These findings reinforce the notion that BL cells are sensitive to oxidative stress (Hockenbery *et al.*, 1990; Falk *et al.*, 1998) and suggest that quantitative and/or functional differences in ROS scavenger enzymes and bcl-2 expression may, at least in part, explain the differential sensitivity of BL cell lines to Ro 40-8757-induced apoptosis. Moreover, our results also indicate that free-radical-producing agents such as Ro 40-8757 in combination with inhibitors of scavenger enzymes may be a promising approach to the selective killing of BL cells *in vivo*.

Materials and methods

Reagents

The arotinoid mofarotene (Ro 40-8757), kindly provided by Dr W Bollag (Hoffman-LaRoche, Basel, Switzerland), was dissolved in DMSO at 0.01 M and diluted in the culture medium so that the final concentration of the solvent was <0.1% (v/v). The stock solutions were stored at -20°C protected from light and oxygen. PDTTC, TTFA, and 2-ME were purchased by Sigma Chemical Co (St. Louis, MO, USA) and dissolved in DMSO. NAC was dissolved in PBS.

Cell lines, patient samples and culture conditions

The BL cell lines used were: Akata, DG75, Namalwa, Daudi, Raji, BL41, P3HR1, and Ramos. The BL41-B95.8 convertant cell line was kindly provided by Dr M Allday (Ludwig Institute for Cancer Research, London). Establishment and characterization of the HDE-14 LCL have been described elsewhere (Pomponi *et al.*, 1996). BJAB cells transfected with the pIgLMP-1 plasmid and the vector alone (Xu *et al.*, 2000) were kindly provided by Dr J Menezés (University of Montreal, Canada). Cell lines were cultured in RPMI 1640 supplemented with 10% heat-inactivated fetal calf serum, 100 U/ml penicillin, 100 µg/ml streptomycin, and 20 mM L-glutamine, and maintained in a humidified 5% CO₂ incubator at 37°C. Short-term BL-cell cultures were obtained from peripheral blood mononucleated cells of CS, a patient with histologically-proven BL in the leukemic phase. The

patient had been off treatment for more than 30 days at the time of sample procurement and gave his/her informed consent to participate in the study. The percentage of CD19⁺, CD10⁺ Igλ⁺ cells in the mononuclear fraction was higher than 90%, and no additional non-B-cell depletion was performed.

Cell proliferation assay

Proliferation assays were performed in 96-well plates in quadruplicate cultures. Cells were seeded at an initial density of 10⁴ cells per well in 200 µl of medium. Experiments with primary BL cells were carried out by seeding 2 × 10⁴ cells per well. At the time points indicated, cultures were pulsed with 1 µCi [³H] methyl thymidine (specific activity 5 Ci/mM; Amersham International, Bucks, UK) for 6 h and subsequently harvested on Unifilter™-96, GF/C™ filter plates (Packard, Meriden, CT, USA). Radioactivity was measured with a liquid scintillation counter (Top Count NXT™, Packard) and results were expressed as mean counts per minute (cpm) ± s.d. of quadruplicate wells. In some experiments, proliferation was also evaluated by counting the number of viable cells (nine aliquots per time point) in a Bürker chamber in the presence of trypan blue.

Cell cycle analysis

The influence of retinoids on cell cycle parameters was investigated by flow cytometry after PI staining. To record a DNA histogram, about 10⁶ cells were pelleted, washed once with PBS, and fixed with 1 ml ice-cold ethanol 70% for 25 min. Cells were then extensively washed from fixative and resuspended for 30 min at room temperature in 1 ml 50 µg/ml PI in 0.1% sodium citrate, 0.01% Nonidet, and 0.01 mg/ml ribonuclease A. Cells were then measured immediately using a FACScan (Becton Dickinson, Mountain View, CA, USA): the excitation wavelength in the cytometer was 488 nm and red (610 nm) fluorescence was recorded. Data acquisition (10⁴ events for each sample) and analysis were performed using the CELLFIT software (Becton Dickinson).

BrdU labeling

Cells were exposed to 10 µM BrdU (Sigma) in growing medium for 30 min at 37°C. After two washes with PBS containing 1% BSA, cells were fixed with ice-cold 70% ethanol for 30 min, centrifuged, and the supernatant was removed. The pellet was resuspended in the denaturing solution (2N HCL/0.5% Triton X-100) at room temperature for an additional 30 min; after centrifugation, 0.1 M Na₂B₄O₇ · 10H₂O (pH 8.5) was added to neutralize the acid and washed out. The cells were resuspended in 0.5% Tween 20/1% BSA/PBS plus primary antibody anti-BrdU (Becton Dickinson) for 30 min at room temperature. After centrifugation, the same buffer plus secondary antibody FITC-conjugated goat anti-mouse Ig (Becton Dickinson) was added for another 30 min incubation. After centrifugation, the pellet was resuspended in PBS containing 5 µg/ml PI and analyzed by flow cytometry. For pulse-chase experiments, 10 µM BrdU were added to the growing medium for a 30-min labeling period at 37°C (pulse), then cell cultures were washed twice and refed with fresh growth medium without BrdU. After a further incubation period (chase), the cells were washed and treated as described before. The relative movement (RM) has been calculated as follows: $RM = \frac{F_S - F_{G1}}{F_{G2} - F_{G1}}$, where F is the mean of red fluorescence of the indicated cell cycle phases. The analysis was carried out at 0, 3, 5, 7, 9, and 12 h. Quantitatively, the time of DNA synthesis (T_S) was

obtained by a graphic representation in which X- and Y-axis were time and RM, respectively.

Apoptosis detection

Apoptosis was evaluated by three different approaches. The first method consisted of fluorescence analysis after PI staining: cell samples were processed as described for cell cycle analysis, and apoptotic populations were investigated by flow cytometry as previously reported (Pomponi *et al.*, 1996). The second method was nick translation labeling of DNA strand breaks (TUNEL): 10^6 cells were washed twice in PBS/1% BSA at 4°C, fixed with 4% paraformaldehyde in PBS (pH 7.4) for 30 min at room temperature, washed with PBS, and permeabilized with 0.1% Triton X-100 in 0.1% sodium citrate for 2 min on ice. After extensive washing, cells were incubated in 50 μ l TUNEL reaction mixture (Boehringer Mannheim, Germany) for 60 min at 37°C in a humidified atmosphere in the dark. Cells were then washed twice, resuspended in PBS and evaluated by flow cytometry. Cells treated with DNase I (10 μ g/ml) for 10 min at room temperature were used as positive controls. The third method consisted of labeling of membrane phosphatidylserine residues by Annexin V: 10^6 cells were collected, washed in PBS, and incubated 15 min with 1 μ g/ml FITC-conjugated Annexin V (Clontech, Palo Alto, CA, USA), with or without PI (2.5 μ g/ml). Under these conditions, PI stains almost exclusively necrotic or late apoptotic cells, while being excluded by normal and early apoptotic cells. Bivariate evaluation of green fluorescence (identifying Annexin-labeled cells) vs red fluorescence (identifying PI-labeled cells) was carried out by flow cytometric analysis.

Analysis of mitochondrial transmembrane potential

The effects of Ro 40-8757 on mitochondrial transmembrane potential were investigated using the fluorescence-based ApoAlert™ Mitochondrial Membrane Sensor kit (Clontech). The assay is based on the use of a cationic dye (MitoSensor™), which, in healthy cells, is taken up in the mitochondria where it forms aggregates exhibiting red fluorescence. In apoptotic cells, alterations in mitochondrial transmembrane potentials prevent the aggregation of the probe in the mitochondria. As a result, the dye remains in monomeric form in the cytoplasm, where it fluoresces green. The fluorescence emitted by the cells was analyzed by flow cytometry.

Caspase activity

Activity of caspase-3(-like) and caspase-9 was analyzed using colorimetric (CPP32/Caspase-3 Assay Kit, Clontech, Palo Alto, CA, USA) and fluorimetric (Caspase-9/6 Fluorescent Assay Kit, Clontech) protease assay kits according to the manufacturer's instructions. Active caspase-3 cleaves the DEVD-pNA substrate, which releases chromophore pNA for spectrophotometric detection, whereas active caspase-9 cleaves the LEHD-AMC substrate, which releases free fluorescent AMC for fluorimetric detection (380-nm excitation filter and 460-nm emission filter). To confirm the specificity of caspase-3 and -9 activation, the CPP32 inhibitor DEVD-fmk and the caspase-9 inhibitor LEHD-CHO were added before incubation with the substrate.

Measurement of ATP

Intracellular ATP levels were determined luminometrically using the luciferin-luciferase method (ATPLite-M kit, Packard). The ATP content was calculated using an external

standard curve and each sample count was normalized on live cells obtained with the trypan blue staining.

Lactate assay

L-lactic acid was determined in the culture media using a commercial kit (Sigma). Results are expressed in μ g/ 10^6 cells.

Measurement of ROS production

ROS generation was measured using a previously established flow cytometry technique based on the superoxide-induced conversion of the oxidant-sensitive dye, dihydroethidine (DHE) (Molecular Probes, Eugene, OR, USA) to ethidium (Rothe and Valet, 1990). Cells were incubated at 37°C for 15 min in the presence of DHE (20 ng/ml, fluorescence at 600 nm) in a complete medium and then immediately analyzed for fluorochrome incorporation by flow cytometry. Production of ROS was also confirmed by using the oxidation-sensitive fluorescent dye 5-(and-6)-chloromethyl-2', 7'-dichlorodihydrofluorescein diacetate (CM-H₂DCFDA, Molecular Probes) (Nishikawa *et al.*, 2000). This probe is first accumulated and hydrolyzed by cytoplasmic esterases of live cells, then it becomes fluorescent when oxidized by ROS.

Northern blotting

Total RNA was isolated using the guanidinium isothiocyanate method (Chomczynski and Sacchi, 1987). RNA samples (15 μ g) were electrophoresed in 1% agarose gels containing 2.2 M formaldehyde, transferred to Pall Biodyne B membranes (Pall, Portsmouth, England) by electroblotting, and baked for 2 h at 80°C *in vacuo*. Hybridizations were performed at 37°C for 18 h in a buffer containing 50% formamide with a [α -³²P] dCTP-labeled probe specific for the NADH dehydrogenase subunit 1 (ND1) gene labeled with [α -³²P] dCTP. The ND1 cDNA probe was obtained from the HDE-14 LCL by RT-PCR using the following primers: 5'-CAC TAT TCC CAC CTC TCC AAT-3' (sense) and 5'-TCG TAA GGG GGA GTT TGG TTA-3' (antisense). PCR conditions were as follows: denaturation at 94°C for 1 min, and annealing at 54°C for 1 min and 72°C for 1 min (35 cycles). Specificity of the ND1 cDNA probe (490 bp) was confirmed by direct sequencing. After hybridization, membranes were washed twice for 5 min in 2 \times standard saline citrate (SSC) at room temperature, twice for 30 min in 2 \times SSC-1% SDS at 65°C, and twice for 30 min in 0.1 \times SSC at room temperature. The filters were then autoradiographed using intensifying screens at -70°C. Sedimentation values of 28S and 18S were used as an internal standard for RNA integrity and loading. Levels of gene expression were determined by densitometric scanning (Bio Rad GS-670, Milan, Italy).

Western blotting

Whole cell extracts were prepared by lysing 10^7 cells in a buffer containing 50 mM Tris-HCl pH 7.5, 150 mM NaCl, 2 mM EDTA, 2 mM EGTA, 25 mM NaF, 25 mM β -glycerolphosphate, 0.1 mM sodium orthovanadate, 0.1 mM phenylmethylsulfonyl fluoride, 5 μ g/ml leupeptin, 1 μ g/ml aprotinin, 0.2% Triton-X-100, and 0.3% Nonidet P-40 (lysis buffer). After 20 min of incubation at 0°C, the extracts were centrifuged for 30 min at 12 000 r.p.m. at 4°C. The protein concentration in the lysate was determined by the Bio-Rad protein assay kit (Bio-Rad Laboratories, Richmond, CA, USA). Aliquots of the supernatant were mixed with 2 \times SDS sample buffer (150 mM Tris-30% glycerol-3% SDS-1.5 mg/100 ml bromophenol blue dye-100 mM DTT) and denatured at 100°C for 5 min. Equivalent

amounts (40 µg) of protein were separated on 12.5% SDS-PAGE and transferred onto nitrocellulose membrane (Schleicher and Schuell, Keene, NH, USA). Ponceau S staining was performed to confirm that equal amounts of total protein were present in all the lanes. The membrane was blocked with 0.5% casein in PBS for 1 h at room temperature and incubated with the appropriate antibody overnight at 4°C. After three washes with 0.5% casein for 5 min, the membranes were incubated for 1 h at room temperature with an appropriate horseradish peroxidase-linked secondary antibody (1:1000). Final washes were performed in 0.5% casein for 15 min, PBS-Tryton X-100 for 5 min (3 times) and distilled water for 5 min. Immunolabeled bands were detected with the ECL Western blotting detection system (Amersham). The antibodies used were: a rabbit polyclonal antibody specific for human ND1 (Pettus *et al.*, 2000) (1:500), kindly provided by Dr JT Greenamyre (Atlanta, GA, USA); anti-CDK4 (H-22, 1:1000), from Santa

Cruz Technologies (Santa Cruz, CA, USA); anti-bcl-2 (clone 124, Dako, Milan, Italy); anti- α -tubulin (clone B-5-1-2, Sigma-Aldrich, Milan, Italy); and anti-LMP-1 (clone S12).

Acknowledgements

This work was supported in part by grants from the Italian Association for Cancer Research (AIRC) (to R.D.) and from MIUR, Progetto Strategico "Oncologia" (SP/4), Legge 449/97, No. 02.00268.ST97. The authors thank Dr Werner Bollag (Hoffmann-La Roche S.p.A.) for supplying Ro 40-8757, Dr J Menezés for providing the LMP-1-transfected BJAB cells and the S12 antibody, Dr JT Greenamyre for the kind gift of anti-ND1 antibody; and Dr P Tonel and Mrs P Pistello for help with the manuscript. PZ and RC are recipients of fellowships from the Italian Foundation for Cancer Research (FIRC)

References

- Barrientos A and Moraes CT. (1999). *J. Biol. Chem.*, **274**, 16188–16197.
- Buttke TM and Sandstrom PA. (1994). *Immunol. Today*, **15**, 7–10.
- Cariati R, Zancai P, Quaiá M, Cutrona G, Giannini F, Rizzo S, Boiocchi M, Dolcetti R. (2000). *Int. J. Cancer*, **86**, 375–384.
- Castleberry RP, Emanuel PD, Zuckerman KS, Cohn S, Strauss L, Byrd RL, Homans A, Chaffee S, Nitschke R and Gualtieri RJ. (1994). *N. Engl. J. Med.*, **331**, 1680–1684.
- Chomczynski P and Sacchi N. (1987). *Anal. Biochem.*, **162**, 156–159.
- Eliason JF, Baumgartner M, Yoshikubo T, Hirabayashi Y, Mitsui H and Inoue T. (1995). *Blood*, **86**, 4516–4526.
- Eliason JF, Inoue T, Kubota A, Horii I and Hartmann D. (1994). *Int. J. Cancer*, **57**, 192–197.
- Eliason JF, Kaufmann F, Tanaka T and Tsukaguchi T. (1993). *Br. J. Cancer*, **67**, 1293–1298.
- Falk MH, Meier T, Issels RD, Brielmeier M, Scheffer B and Bornkamm GW. (1998). *Int. J. Cancer*, **75**, 620–625.
- Fenaux P, Chomienne C and Degos L. (1997). *Semin Oncol.*, **24**, 92–102.
- French LE, Ramelet AA and Saurat J-H. (1994). *Lancet*, **344**, 686–687.
- Fridovich I. (1995). *Annu. Rev. Biochem.*, **64**, 97–112.
- Hartmann D, Teilmann K, Eliason J, Kaufmann F and Klaus M. (1993). *Retinoids: Progress in Research and Clinical Applications*. Livrea MA, Packer L (eds). Marcel Dekker: New York, NY, pp. 491–502.
- Hecht JL and Aster JC. (2000). *J. Clin. Oncol.*, **18**, 3707–3721.
- Henderson S, Rowe M, Gregory C, Croom-Carter D, Wang F, Longnecker R, Kieff E and Rickinson A. (1991). *Cell*, **65**, 1107–1115.
- Higuchi M, Proske RJ and Yeh ETH. (1998). *Oncogene*, **17**, 2515–2524.
- Hockenbery D, Nunez G, Millman C, Schreiber RD and Korsmeyer SJ. (1990). *Nature*, **348**, 334–336.
- Huang P, Feng L, Oldham EA, Keating MJ and Plunkett W. (2000). *Nature*, **407**, 390–395.
- Knowles DM, Chamulak GA, Subar M, Burke JS, Dugan M, Wernz J, Slywotzky C, Pelicci G, Dalla-Favera R and Raphael B. (1988). *Ann. Intern. Med.*, **108**, 744–753.
- Komano J, Maruo S, Kurozumi K, Oda T and Takada K. (1999). *J. Virol.*, **73**, 9827–9831.
- Kroemer G and Reed JC. (2000). *Nat. Med.*, **6**, 1067–1074.
- Louvet C, Djelloul S, Forgue-Lafitte M-E, Mester J, Zimmer A and Gespach C. (1996). *Br. J. Cancer*, **74**, 394–399.
- Marton A, Mihalik R, Bratincák A, Adleff V, Petak I, Vegh M, Bauer PI and Krajcsi P. (1997). *Eur. J. Biochem.*, **250**, 467–475.
- Morrison VA and Peterson BA. (1999). *Semin. Oncol.*, **26**, 84–98.
- Nishikawa T, Edelstein D, Du XL, Yamagishi S, Matsumura T, Kaneda Y, Yorek MA, Beebe D, Oates PJ, Hammes HP, Giardino I and Brownlee M. (2000). *Nature*, **404**, 787–790.
- Ohno R. (1994). *Leuk. Lymph.*, **14**, 401–409.
- Pettus EH, Betarbet R, Cottrell B, Wallace DC, Madyastha V and Greenamyre JT. (2000). *J. Neurochem.*, **75**, 383–392.
- Pitkanen S and Robinson BH. (1996). *J. Clin. Invest.*, **98**, 345–351.
- Pomponi F, Cariati R, Zancai P, De Paoli P, Rizzo S, Tedeschi RM, Pivetta B, De Vita S, Boiocchi M and Dolcetti R. (1996). *Blood*, **88**, 3147–3159.
- Pryor WA. (1982). *Ann. N.Y. Acad. Sci.*, **393**, 1–22.
- Richter C and Schweizer M. (1997). *Oxidative Stress and the Molecular Biology of Antioxidant Defenses*. In: Scandalios JG (ed). Cold Spring Harbor Laboratory Press: Plainview, NY, pp. 169–200.
- Richter C, Schweitzer M, Cossarizza A and Franceschi C. (1996). *FEBS Lett.*, **378**, 107–110.
- Rothe G and Valet G. (1990). *J. Leukoc. Biol.*, **47**, 440–448.
- Ruf IK, Rhyne PW, Yang C, Cleveland JL and Sample JT. (2000). *J. Virol.*, **74**, 10223–10228.
- Seaton TA, Cooper JM and Schapira AHV. (1998). *Brain Res.*, **809**, 12–17.
- Slater AF, Nobel CS and Orrenius S. (1995). *Biochim. Biophys. Acta*, **1271**, 59–62.
- Teilmann K, Tsukaguchi T, Klaus M and Eliason JF. (1993). *Cancer Res.*, **53**, 2319–2325.
- Uchida T, Inagaki N, Furuichi Y and Eliason JF. (1994). *Int. J. Cancer*, **58**, 891–897.
- White L, Siegel SE and Quah TC. (1992). *Crit. Rev. Oncol. Hematol.*, **13**, 55–71.
- Xu J, Ahmad A, D'Addario M, Knafo L, Jones JF, Prasad U, Dolcetti R, Vaccher E and Menezes J. (2000). *J. Immunol.*, **164**, 2815–2822.